ELSEVIER

Carbohydrate Research 300 (1997) 19–29

CARBOHYDRATE RESEARCH

An NMR study of the dynamic single-stranded conformation of sodium pectate

Laurent Catoire [a], Christiane Derouet [a], Anne-Marie Redon [a], Renée Goldberg [b], Catherine Hervé du Penhoat [a,*]

[a] *URA CNRS 1679, Département de Chimie, Ecole Normale Supérieure, 75231 Paris Cedex 05, France*

[b] *Laboratoire d'Enzymologie en Milieu Structuré, Institut Jacques Monod, 2 Place Jussieu, 75251 Paris, France*

Received 4 November 1996; accepted 24 January 1997

Abstract

The conformation of aqueous sodium pectate has been probed by fitting multi-field experimental ^{13}C NMR relaxation data with various expressions for the spectral densities. The model-free, DLM, and diffusion-in-a-cone spectral densities all reproduced the experimental data in a reasonable manner. The validity of the resulting motional models was evaluated by comparison to data obtained from hydrodynamic theory and molecular modeling. The diffusion-in-a-cone spectral densities afforded both the best fit to experimental data and the most precise description of secondary structure. The optimum motional model could be described as anisotropic reorientation of two-fold helical segments containing 29 residues. The corresponding average axial length of the helical segments of 13 nm is in excellent agreement with the persistence length from small-angle neutron scattering and molecular mechanics. The transverse or hydrodynamic radius of the helical segments was 0.8 nm as compared to a covalent radius of 0.4–0.45 nm. The increase in hydrodynamic radius with respect to the covalent radius indicated significant counterion condensation in keeping with polyelectrolyte theory. © 1997 Elsevier Science Ltd.

Keywords: ^{13}C NMR relaxation; Secondary structure; Conformation; Hydrodynamic radius; Sodium pectate; Polysaccharide; Polyelectrolyte

1. Introduction

Pectins are a family of complex anionic polysaccharides that constitute as much as a third of the dry weight of plant primary cell walls. These biopolymers consist primarily of α-(1 → 4)-linked D-galacturonyl sugars interrupted by (1 → 2)-linked α-L-rhamnopyranosyl residues. The homogalacturonan parts of the polymer are referred to as 'smooth' regions while the rhamnose-rich zones are called 'hairy' regions as the latter sugars carry neutral oligosaccharide side-chains frequently composed of D-Gal*p* and L-Ara*f* sugars (Fig. 1). In native pectins about 70% of the galacturonan carboxyl groups are methylated. Besides their structural and functional

* Corresponding author. Fax: +33-0144322402.

PII S0008-6215(97)00035-9

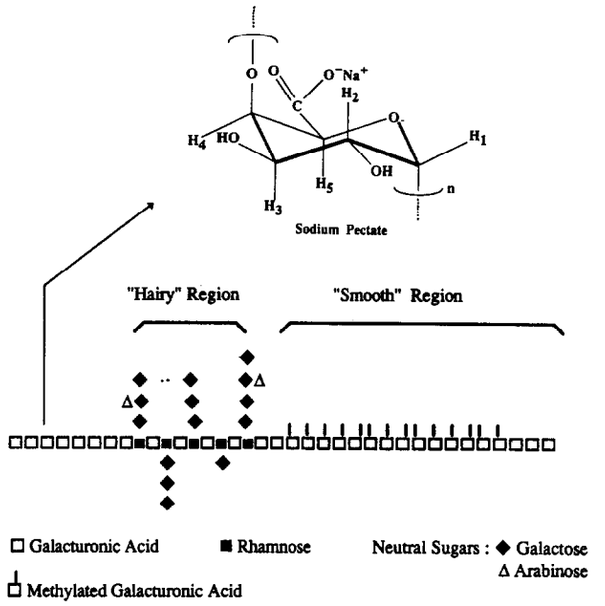

Fig. 1. Schematic drawing of pectin (rhamnogalacturonan I) showing the smooth and hairy regions. The formula for sodium pectate, a model for the homogalacturonan region, is given above.

roles in higher plants [1], these macromolecules are extensively used as gel formers and thickening agents in the food industry [2]. Although the primary structure of pectins has been widely studied, an overall picture of the secondary, tertiary, and quaternary structures in gels or in solution has not yet emerged [3,4].

Experimental probes of pectin structure have been obtained both for the solid- (transmission electron microscopy or TEM [4], fiber-diffraction [5], and atomic force microscopy or AFM [6]) and liquid-state (light-scattering [7], viscosimetry [8], ^{23}Na NMR [9], potentiometry and circular dichroism [8,10], small-angle neutron scattering or SANS [3]). A considerable range of persistence lengths, L_p, has been described on the basis of solution-state experimental data (4.5–40 nm). However, direct comparison of results obtained for samples of different origin is hazardous, as many factors such as concentration, ionic strength, degree of methylation, and percentage of rhamnose residues (i.e. side-chain oligosaccharides) have been shown to influence the conformational behaviour and/or hydrodynamic properties of pectin [3,7].

Molecular mechanics (MM) studies of homogalacturonans [3] and fiber-diffraction analyses [5], have indicated that conformations corresponding to both two- and three-fold (right- and left-handed) helices represent favourable modes of chain propagation. This theoretical approach, which suggested that four-fold helical structures would also be energetically viable, showed that the pitch (rise per residue) for all these helices was close to 0.443 nm. The persistence lengths obtained in these simulations were much shorter (13.5 nm) than those (40 nm) described in the pioneering work of Burton and Brant [11]. No significant influence of either the methoxy groups or the rhamnose residues upon chain dimension was observed with the MM3 approach. As experimental data point to a marked effect of these structural features upon macroscopic properties, it could be surmised that some factors had not been accounted for in the theoretical studies. Indeed, the glycosidic orientations of the galacturonosyl sugars in the theoretical polymers, which determine secondary structure, were based on results from MM studies of model disaccharides [12] for which only next-neighbour interactions can occur. However, the variations in the macroscopic properties with structural modifications could also be the result of changes in tertiary or quaternary structure (often referred to as junction zones [13] or entanglement networks [14]). Finally, in another theoretical study of a galacturonan fragment (12 residues) based on condensed-phase molecular dynamics simulations (MD) in the presence of counterions, stable conformers with a more loosely coiled helical secondary structure were reported [15].

^{13}C NMR relaxation data allow the characterization of motion at the molecular level and provide the basic connectivity between primary structure and hydrodynamic properties of macromolecules [16]. Although the dynamic properties of the gel-state are of greater practical importance, relaxation studies on dilute solution provide valuable information on the intramolecular motional processes. The helical conformation of pectic fragments is of interest in its own right, as related oligosaccharides have been shown to be signaling molecules [17]. Liquid-state relaxation data not only characterize the nature, amplitude, and timescales of local, segmental, and eventually overall motion but, as they probe the hydrodynamic radius of the macromolecule, they might lead also to a description of solvation.

The study of carbohydrate dynamics with ^{13}C relaxation data has been reviewed recently [18]. In the case of polysaccharides, relaxation data have occasionally been simulated with the model-free approach associated with isotropic molecular reorientation [19,20]. However, generally speaking, fitting of the carbon relaxation data of carbohydrate polymers

(low-molecular-weight polysaccharides [21], glycopolymers [22], and high-molecular-weight polysaccharides [23]) has required spectral densities which correspond to anisotropic overall tumbling. The most extensively studied polysaccharide, amylose, has been analyzed with various detailed physical models [23–25] (the more successful models being diffusion-in-a-cone [26], a two-state jump model [27], and the DLM model [28] which contains both diffusive [29] and jump types of motion [30]). The most satisfying simulation of the methine carbon relaxation data over a wide range of temperatures was achieved with the DLM model [25].

As a first step towards understanding the conformational preferences of pectins through NMR relaxation data, we undertook the study of sodium pectate. This macromolecule can be obtained in a single coil conformation in solution at acceptable concentrations for NMR spectroscopy and it represents a good model for the de-esterified 'smooth regions' of pectins.

2. Experimental

Sample preparation.—The schematic drawing of sodium pectate with labels for the proton atoms has been given in Fig. 1. A sealed tube for the NMR study was prepared by dissolving 25 mg of polygalacturonic acid (Sigma) and 1 equiv NaOH in 1 mL D_2O (99.96%). The sample was degassed using 5 freeze–thaw cycles under argon to remove dissolved oxygen and other gases. The pH of the resulting soln was close to 5.

Viscosity measurements.—Viscosity measurements were performed on solns of sodium pectate with a Cannon–Manning Semi-micro viscometer at 25 ± 0.1 °C in 2.5 mM NaCl.

^{13}C NMR relaxation experiments.—All NMR measurements were conducted at 294 K on Bruker spectrometers (AC200, AC250, and AM400) operating in the FT mode. Spin–lattice relaxation times were measured with the inversion–recovery sequence. The recycle time was greater than $6 \times T_1$ and data were collected for 10 τ values which varied from 6 ms to $2 \times T_1$. The intensities of the peaks were fitted to a three-parameter exponential function using spectrometer system software. Experiments were run at least twice. Spin–spin relaxation times were obtained by measurement of the half-height linewidth rather than the spin–echo technique. An inhomogeneity contribution was established from the natural linewidth of a reference sample of acetone (< 0.4 Hz). Nuclear Overhauser enhancements (NOEs) were determined by comparison of the integrals of gated decoupled and fully decoupled spectra. A prescan delay of $5 \times T_1$ was used.

Numerical simulations.—Carbon relaxation data (T_1^{-1}, T_2^{-1}, and NOE) were simulated using in-house software (RELAX). The general expressions for the relaxation parameters as a function of the spectral densities were taken from ref. [31], and the exact spectral density functions for the various models were those given in the original papers. The various assumptions concerning the expressions for the spectral densities (isotropic or anisotropic overall tumbling, independence of the contributions of overall and internal motion etc.) have been discussed both in the original reports and in ref. [23]. These theoretical data were least-squares fitted to the experimental data using two versions [32,33] of the SIMPLEX algorithm [34]. This protocol was similar to the one described by Levy et al. [35] (MOLDYN program), but in the present case, the linewidth data have not been normalized with respect to the T_1 and NOE data. In the case of polysaccharides, overall motion is too slow to effect T_1 and NOE data and only T_2 data are influenced by the longer correlation times [through the $J(0)$ term]. Moreover, it has been shown [22,23] that inappropriate models generally fail to reproduce T_2 data of polysaccharides while they may lead to reasonable values for T_1 and NOE data. The relative values for T_1^{-1} (dashed curve), T_2^{-1} (solid curve), and η (dotted curve) have been traced in Fig. 2. In order to avoid meaningless simulations, no weighting functions were added to the optimization routine, and therefore only models which could reproduce the T_2 data would be expected to converge.

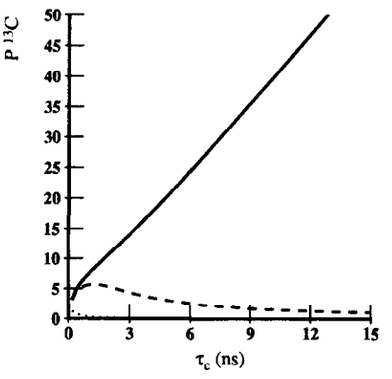

Fig. 2. Plots of ^{13}C relaxation parameters (P ^{13}C) as a function of overall tumbling (ns) for a rigid rotor. T_1^{-1}, T_2^{-1}, and heteronuclear NOEs are represented by dashed, solid, and dotted curves, respectively.

3. Results and discussion

The general approach adopted in the present study consisted in first establishing the correlation times (τ_z and $\tau_x = \tau_y$) for segments of sodium pectate of various lengths and helical radii from hydrodynamic theory. Geometric parameters (angles between C–H vectors and molecular axes) for helical segments of varying symmetry (two-, three-, and four-fold axes) were assessed from the optimized structures [3] generated with the polysaccharide generator algorithm POLYS [36]. In a second step, the experimental carbon relaxation parameters (T_1^{-1}, T_2^{-1}, and heteronuclear NOEs) were least-squares fitted to theoretical data established for physical models of increasing complexity. The various dynamic (correlation times and order parameters) and geometric (angles between C–H vectors and molecular axes) parameters of the theoretical motional models were treated as adjustable parameters in this protocol. These simulations resulted in an *experimental NMR motional model*. In a third step, the data obtained from hydrodynamic theory or molecular mechanics and NMR were compared to discriminate between physically realistic and unrealistic *experimental NMR motional models*. Finally, the information content and the uniqueness of the NMR-derived dynamic models was discussed.

Motional and geometric parameters of sodium pectate from hydrodynamic theory and molecular modeling.—The overall tumbling time of the sodium pectate sample was evaluated independently from hydrodynamic theory for both the isotropic and anisotropic cases. Accordingly, the intrinsic viscosity was measured in 2.5 mM NaCl at 298 K and found to be 0.62 dL/g. The weight-average molecular weight (M_w) was then determined to be 16,000 Da from the following Mark–Houwink relation [37],

$$[\eta] = 1.4 \times 10^{-6} \times M_w^{1.34} \quad (1)$$

These data are analogous to those ($[\eta] = 0.728$ dL/g and $18{,}400 < M_w < 21{,}000$ Da) determined by Cesaro et al. [8] for sodium pectate prepared from pectic acid of similar origin (Sigma).

In the case of *isotropic molecular reorientation* which can be described by a single correlation time, τ_R°, at infinite dilution, the time constant can be expressed as a function of intrinsic viscosity, $[\eta]$, according to the following [38],

$$\tau_R^\circ = 2M_w[\eta]\eta_o/3RT \quad (2)$$

where η_o is the solvent viscosity. In a solution of a neutral polysaccharide at finite concentration, C, the correlation time, τ_R, is given by the following equation [39]

$$\ln(\tau_R/\tau_R^\circ) = k'[\eta]C \quad (3)$$

However, the viscosity of dilute solutions of polyelectrolytes displays unique dependence on concentration [14] in the limit of zero ionic strenght precluding straightforward measurement of the Huggins constant k'. Nonetheless, a value of 0.4 μs was established for τ_R° at infinite dilution from Eq. (2).

In the event of *anisotropic motion of helical-chain segments*, a cylindrical model with two rotational correlation times, one for diffusion about the major axis (z-axis) [40] and one for diffusion about the minor axis (x-axis) [41], can be used to describe the hydrodynamic behaviour as follows,

$$\tau_z = 8\pi\eta_o b^2 L/6kT \quad (4)$$

$$\tau_x = \pi\eta_o L^3\{\ln(L/b) - 1.57 + 7[1/\ln(L/b) - 0.28]^2\}/18kT \quad (5)$$

where $L = 0.443n$ (nm) is the axial length of the cylinder which depends on the number of residues, n, and the pitch per residue (0.443 nm) of the pectate helix. Finally, b is the transverse or hydrodynamic radius of the cylinder.

This latter parameter was estimated to be about 0.5 nm for sodium pectate in both a ^{23}Na NMR study [9] and in work based on potentiometric methods [8], but a larger value would be expected from polyelectrolyte theory [42], particularly at very low salt concentration. The covalent radius of partially methylated pectins has been estimated to be between 0.3–0.4 nm by small-angle neutron scattering [3]. The ionic radius of sodium in aqueous solutions has been determined to be 0.235 nm [43], and radial pair distribution functions from condensed-phase MD simulations indicate that the -COO$^-$ ligand is located at about 0.25 nm from sodium cations [15]. Therefore, the radius for fully solvated sodium pectate should be between 0.5–0.9 nm, taking into account counterion binding (0–100%). In the case of a 0.4 w/v solution of pectic acid, a rapid increase in the ^{23}Na NMR linewidths indicated appreciable counterion binding at neutralization degrees greater than 0.72.

From counterion condensation theory [44] the linear polyion charge density, ξ, and charge fraction, f, are defined as,

$$\xi = q^2/\varepsilon_o\varepsilon_R kTp \quad (6)$$

and

$$f = (N\xi)^{-1}$$

where q is the protonic charge, ε_0 is the permittivity in a vacuum, ε_R is the permittivity of the solution, p is the linear charge spacing of the polyion, and N is the total charge of the counterion. f Is defined as the ratio of that part of its structural charge which is uncompensated by bound counterions to its total structural charge. The above theory predicts that more than a third (0.38) of the sodium ions are bound to the pectic helix. A value of 0.29 has been reported recently in a study of dilute solutions of sodium pectate under low salt conditions by viscosimetry [45]. Rotational correlation times have been calculated for sodium pectate as a function of the number of residues per helical segment using both 0.5-nm (values in italics) and 0.8-nm values for b, and these data are collected in Table 1.

The appropriate values of the β angle (β is the angle between the C–H vectors and the z-axis) for all the stable pectin helices (right- or left-handed with a two-, three-, or four-fold axis of symmetry) described with molecular mechanics [3,36] were evaluated directly from the cartesian coordinates of the corresponding models. These β values have been plotted as a function of the number of residues per helical turn in Fig. 3. It is noteworthy that the β values of the various C–H vectors are all very different (e.g. 84, 145, 38, 98, 32° for C-1 to C-5, respectively, in a two-fold helix) whereas for a given C–H vector the variation in β in going from a two- to a four-fold helix is not very large (< 20°).

Table 1
Rotational correlation times calculated from hydrodynamic theory [40,41] for helical segments of varying lengths, L, with a transverse radius, b, of either 0.8 nm (above) or 0.5 nm (below in italics)

Number of residues	L (nm)	τ_z (ns)	τ_x (ns)
10	4.4	2.8	5
		1.1	*5*
15	6.6	4.3	16
		1.7	*11*
20	8.9	5.7	30
		2.2	*22*
25	11.1	7.1	52
		2.8	*38*
30	13.3	8.5	77
		3.4	*58*
35	15.5	10	110
		3.9	*84*
40	17.7	11	153
		4.5	*118*
45	19.9	13	202
		5.1	*157*
50	22.1	14	258
		5.6	*204*

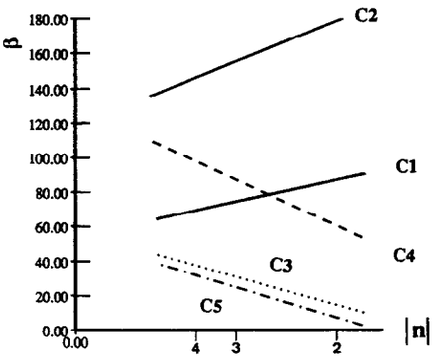

Fig. 3. Plots of the angle between the helix axis and the C–H vectors (β) for methine carbons, C-1 to C-5, as a function of the number of residues per helical turn.

The spatial restriction of internal motion is either expressed as an order parameter (model-free model) or as the half-angle of the cone in which diffusive motion occurs (DLM and diffusion-in-a-cone models). The half-angle representation for the amplitude of internal motion can be compared to S^2 through the corresponding squared cosine ($S^2 \sim 0.25\cos^2\theta°(1 + \cos\theta°)^2$ [46]). S^2 Values of 0.69–0.73 have been calculated for the methine carbons of the α-glucopyranosyl residue of sucrose from a 1-ns condensed-phase MD simulation [47]. Analogous values have been estimated from ^{13}C NMR relaxation data for the C–H vectors of heparin oxide ($S^2 \sim 0.65 M_w \sim$ 12,000 [21]) which also contains an α-(1 → 4) linkage or for those of a larger α-glycopolymer ($S^2 \sim 0.63 M_w \sim 66{,}400$ [22]).

Experimental NMR data.—The experimental carbon T_1, T_2, and heteronuclear NOE values measured at three magnetic field strengths (200, 250, and 400 MHz) are collected in Table 2 along with the average deviations. The T_1 values were reproducible (±5–10%), whereas the precision for the NOEs should in principle be less. In the case of sodium pectate, very homogeneous values for the heteronuclear NOEs were

Table 2
Multi-field ^{13}C relaxation parameters (T_1 and T_2 in ms) and average deviations of a 2.5% w/v of sodium pectate in D_2O at 294 K

Carbon atom	100.6 MHz			62.9 MHz			50.3 MHz		
	T_1 (ms)	T_2 (ms)	NOE	T_1 (ms)	T_2 (ms)	NOE	T_1 (ms)	T_2 (ms)	NOE
C-1	295 ± 12	34 ± 2	1.59 ± 0.06	179 ± 9	32 ± 4	1.73 ± 0.08	156 ± 15	31 ± 4	1.79 ± 0.11
C-2	284 ± 17	28 ± 3	1.43 ± 0.06	168 ± 11	27 ± 4	1.60 ± 0.06	143 ± 12	26 ± 4	1.72 ± 0.09
C-3	296 ± 11	34 ± 2	1.44 ± 0.07	169 ± 15	32 ± 3	1.62 ± 0.09	122 ± 8	31 ± 4	1.75 ± 0.08
C-4	277 ± 14	29 ± 3	1.45 ± 0.06	174 ± 8	27 ± 4	1.63 ± 0.07	150 ± 17	26 ± 5	1.75 ± 0.11
C-5	286 ± 11	33 ± 2	1.47 ± 0.04	169 ± 1	32 ± 3	1.62 ± 0.08	134 ± 14	31 ± 5	1.70 ± 0.12

found (±3–8%), but it must be remembered that the carbon spectrum contained only six well-resolved signals. In contrast, the T_2 values were very short (~ 30 ms) and difficult to measure accurately with the CPMG technique. Consequently, the spin–spin relaxation times were obtained from the measurement of the half-height linewidth (typically 14 Hz at 100.6 MHz) as outlined in the Experimental section. It would have been desirable to conduct the relaxation measurement with the pulse sequences recommended [48,49] for the suppression of the effects of cross-correlation between dipolar and chemical-shift anisotropy relaxation mechanisms. Hricovini and Torri [50] have shown that for a pentasaccharide at 500 MHz, T_1 (T_2) values measured in this way are 10–15% (10–20%) larger than those evaluated with the standard inversion–recovery technique (CPMG). Spectrometer limitations did not allow these determinations, but as the CSA contribution only becomes important at high magnetic field strength, the influence of cross-correlation effects on the relaxation parameters must be small in the present case.

Fitting of ^{13}C NMR data to physical motional models.—Motional models requiring one, three, four, and five adjustable parameters, respectively, were evaluated with respect to their capacity to reproduce the carbon relaxation data of sodium pectate. The rigid rotor, which was the simplest motional model considered, is characterized by a unique correlation time for molecular reorientation, τ_R. The second model, the so-called 'model-free model' [51], includes two correlation times, one for overall tumbling, τ_c, and one for internal motion, τ_e, as well as an order parameter, S^2_{ang}, which describes the spatial restriction of internal motion. In the DLM model [25], the timescale of chain segmental motion is set by two parameters, τ_1 and τ_2, which characterize single and cooperative transitions, respectively. The additional librational motion of the C–H vectors is described in terms of fast anisotropic motion occurring with the correlation time, τ_o, inside a cone of half-angle, $\theta°$, the axis of which coincides with the rest position of the C–H vector. For simplicity, the axis of the librational motion is taken to be the same as that of the segmental motion, but the two types of motion are otherwise independent. Finally, in the diffusion-in-a-cone model [26], internal motion is described as wobbling in a cone, so that the C–H vector moves freely with a correlation time, τ_w, inside the conical boundary defined by an angle $\theta°$. This motion is superposed on the overall motion of a cylindrical segment that is axially symmetrical and characterized by correlation times τ_z (about the major axis) and $\tau_x = \tau_y$ (about the minor axis). β Is the angle that the director of the cone makes with the z-axis (Fig. 4).

The theoretical carbon T_1, T_2, and heteronuclear NOEs (P_i^{calc}) established for C-5 with the preceding models have been collected in Table 3 along with the corresponding experimental data (P_i^{obs}). The fit between the experimental and theoretical data sets (C-1 to C-5) has been quantitatively evaluated through the χ^2 values according to the following expression,

$$\chi^2 = \sum_{i=1}^{N} \left(P_i^{obs} - P_i^{calc}\right)^2$$

Comparison of these values to the summed squares of the experimental average deviations (0.08) allows a quantitative evaluation of the various models. Intuitively, as the number of fitting parameters increases one would expect the quality of the fit to improve unless the dynamic behaviour of sodium pectate could indeed be assimilated to isotropic overall tumbling of a rigid sphere.

The T_2 data are identical for all three models, but it should be remembered that the fit for this relaxation parameter dominates the χ^2 values in our fitting routine. In the case of sodium pectate, the T_2

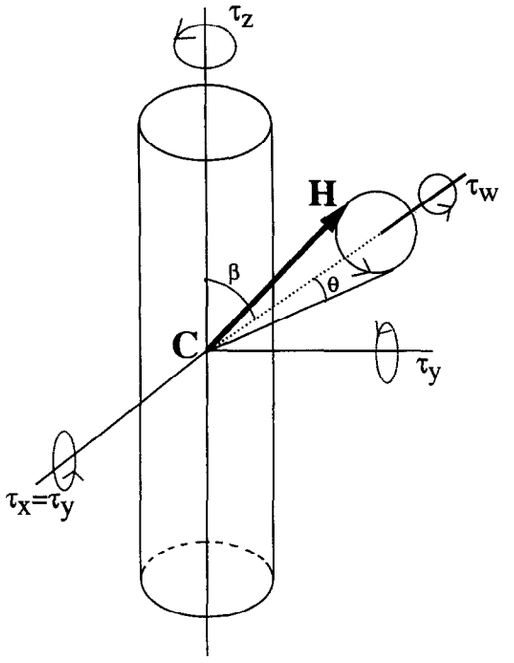

Fig. 4. Diffusion in a cone model.

values do not vary significantly with the magnetic field strength at room temperature, which is characteristic of macromolecules with correlation times ≥ 5 ns (i.e. $T_2 \leq 50$ ms). The rigid rotor model is thus characterized by a correlation time of 7 ± 1 ns, which is necessary to reproduce the T_2 data (Table 4). However, this time constant is almost two orders of magnitude shorter than the correlation time, τ_R^o, calculated for isotropic overall tumbling from hydrodynamic theory. A very poor fit ($\chi^2 = 0.7$) is obtained for this motional model as would be expected in the presence of internal motions and/or anisotropic reorientation. In contrast, the χ^2 values for the other three models indicate that they reproduce the experimental data in a reasonable manner ($\chi^2 \leq$ experimental precision). The T_1 and NOE data are well simulated with the diffusion-in-a-cone ($\chi^2 = 0.005$) model whereas in the case of the model-free model ($\chi^2 = 0.01$) the NOEs at 62.9 and 100.6 MHz are systematically too high. On the whole, the NOE data are too weak with the DLM model ($\chi^2 = 0.04$; C-5 is the carbon with the best fit for this model) which also regularly predicts T_1 values at the highest magnetic field strength that are too low (-0.03 s).

The values of two time constants associated with the model-free simulation are 11 ± 1 and 0.8 ± 0.2 ns, respectively. The second correlation time is required to reproduce the T_1 and NOE data and a unique solution is obtained for all five methine carbons. However, this model is not physically realistic as the order parameters are slightly too low (an average value of 0.57 instead of 0.63–0.73), and the τ_c value (12 ± 2 ns) obviously does not correlate with overall tumbling (roughly 0.4 μs) but must correspond to a more local type of motion or an

Table 3
Comparison of theoretical NMR relaxation parameters for C-5 of sodium pectate for models of increasing complexity (one, three, four, and five adjustable parameters) with the corresponding experimental data (in bold)

Model	Parameters	χ^2	Ref.	Carbon frequency	T_1 (ms)	T_2 (ms)	NOE
Experimental data		8.2E − 2		50.3	**134**	**31**	**1.70**
				62.9	**162**	**32**	**1.62**
				100.6	**286**	**33**	**1.47**
Rigid rotor, overall isotropic motion	τ_R	6.6E − 1		50.3	109	30	1.19
				62.9	160	32	1.17
				100.6	381	34	1.16
'Model-free' isotropic motion, internal motion of amplitude S^2	S^2, τ_c, τ_e	1.1E − 2	[51]	50.3	131	31	1.75
				62.9	171	32	1.70
				100.6	290	34	1.53
DLM	θ, τ_0, τ_1, τ_2	4.1E − 2	[28]	50.3	157	31	1.67[5]
				62.9	178	32	1.62
				100.6	245	33	1.48
Diffusion in a cone	β, θ, τ_w, τ_x, τ_z	4.6E − 3	[26]	50.3	131	31	1.70
				62.9	169	32	1.64
				100.6	286	34	1.46[5]

Table 4
Dynamic and geometric parameters for various spectral density functions obtained by least-squares fitting of the multi-field ^{13}C relaxation data of a 2.5% w/v solution of sodium pectate

Model	Parameter	C-1	C-2	C-3	C-4	C-5	$\bar{x}$
	S^2	0.56	0.59	0.58	0.57	0.58	
'Model-free'	τ_c (ns)	10.9	12.7	10.2	12.8	10.6	12 ± 1
	τ_e (ns)	0.6	0.9	0.8	0.9	0.9	
	θ (°)	43.3	43.4	39.9	43.6	44.7	
DLM	τ_0 (ns)	0.5	0.6	0.7	0.6	0.6	
	τ_1 (ns)	13.5	12.1	7.1	14.4	14.5	11 ± 4
	τ_2 (ns)	73.4	110.3	94.5	102.0	81.0	93 ± 17
	θ (°)	35.6	35.4	35.2	35.4	35.6	
	β (°)	91.9	141.5	33.5	90.1	29.8	
	C_n	2	2	2	2	2	
Diffusion in a cone	τ_w (ns)	1.0	1.6	1.6	1.6	1.4	
	τ_z (ns)	5.2	11.0	8.8	6.3	9.7	8 ± 3
	τ_x (ns)	67.9	72.5	56.5	64.6	66.4	62 ± 6
	b (nm)	0.60	0.95	0.9	0.7	0.9	0.8 ± 0.2
	n	32	27	26	29	27	29 ± 3

apparent τ_c. In the case of the DLM model, convergence requires motion on three well-separated timescales. The values of the τ_1, τ_2, and τ_0 correlation times are 90 ± 20, 11 ± 4, and 0.6 ± 0.1 ns, respectively. In the DLM model, the τ_1 value corresponds to single (or uncompensated) transitions, and from the data in Table 1 it would appear that such motion can be assimilated to rotation about the minor axis of helical segments. However, here the diffusive type of motion is even less restricted as the corresponding average order parameter would be 0.40, and therefore this motional model must be rejected.

Finally, the diffusion-in-a-cone model also leads to three time constants that are very different (62 ± 6, 8 ± 3, and 1.4 ± 0.2 ns for τ_x, τ_z, and τ_w, respectively; Table 4). The first two motional parameters are compatible with the correlation times established from hydrodynamic theory (Table 1) for a helical segment of about 29 residues and a hydrodynamic radius of 0.8 ± 0.2 nm. In this case, the amplitude of the diffusive motion of the C–H vectors (an average order parameter of 0.56) is also slightly too low. The β values simulated with this model were all within $\pm 14°$ of those established for the theoretical two-fold helix [3]. Although motional models which corresponded to helical segments with a four-fold symmetry axis also reproduced the relaxation data in the case of certain carbons such as C-5, only the model in Table 4 was satisfactory for the anomeric carbon. The corresponding average axial length of the helical segments was 13 nm, in excellent agreement with the persistence length from small-angle neutron scattering and molecular mechanics [3]. It is interesting to note that although sodium ions bound to pectate have been detected by ^{23}Na NMR, a corresponding increase in the hydrodynamic radius of sodium pectate has not been clearly demonstrated in prior work. Indeed, the hydrodynamic radius established from the ^{13}C relaxation data suggest that a major fraction of the sodium ions are bound to the polymer, in agreement with Manning's counterion condensation theory (38%).

The spectral densities are maximum for motion occurring on a timescale close to the reciprocal of the corresponding transition frequencies. As a result, correlation times in the 0.3–3 ns range are expected to be fairly well defined in the present study whereas those of slower motion [which is only probed by the $J(0)$ term in the T_2 expression] or faster motion should be much less accurate. Four fairly distinct timescales for molecular fluctuations have been described in simulations of the ^{13}C relaxation data of polysaccharides: 20–90 [21,22,25], 3–15 [23,25], 0.6–2.0 [18,21–23,25], and 0.05–0.15 ns [18,21–23,25]. The two longest correlation times are found with models based on anisotropic reorientation and characterize the end-over-end motion of either helical segments or the entire molecule and rotation about the helical axis, respectively. The third or nanosecond timescale has been imputed to overall motion (isotropic tumbling), rotation about the helical axis (anisotropic tumbling), diffusive internal motion, and

cooperative jump-type fluctuations. The most rapid motion is attributed to small-amplitude uncorrelated dihedral fluctuations (model-free formalism [51]). It seems reasonable to postulate that all these timescales are necessary to reconstitute the time correlation functions (TCF) of polysaccharides.

The greater efficiency of motion in the 0.3–3 ns range in modulating relaxation suggests that cooperative or correlated motion on the nanosecond timescale must be represented to obtain physically realistic motional models. Monitoring the correlation function during MD simulations shows that ring breathing (6–7° rms fluctuation; 20° maximum fluctuation [52]) associated with small-amplitude glycosidic transitions (20° rms fluctuation [47]) may represent an alternative mode of cooperative motion to large-amplitude glycosidic transitions (interwell). In the future, an explicit TCF for carbohydrate chains [25] or the orientational TCF for local dynamics developed by Perico [53] may reveal the precise nature of this cooperative motion that modulates nuclear spin relaxation in carbohydrates.

Interpretation of the NMR-derived motional model. —Polysaccharides are known [54] to present heterogeneous macroscopic conformation, including single-stranded regions and junction zones [13] or entanglement networks [14]. As the preceding relaxation study would only characterize the former form, it was necessary to determine to what extent multi-stranded and aggregated species (helix–helix associations) coexisted with the single-stranded helical segments. Variable-temperature ^{13}C NMR studies of sodium pectate have shown [10] that aggregated or multi-stranded species are not detected at room temperature. The 2.5% (w/v) sample used for relaxation measurements was not turbid, but the presence of aggregated species could not be ruled out. Accordingly, an inverse-gated spectrum of a sample containing an internal standard (sucrose) was recorded, and the extent of aggregation was estimated to be $\leq 10\%$. A rapid calculation showed that the total volume occupied by the macromolecule was $\sim 10\%$, and hence entanglement networks would not be expected under these conditions [14].

Rees and co-workers [55,56] have shown that a minimum of 14 residues are required for cooperative formation of junction zones in the presence of calcium ions. As binding to sodium counterions is weaker, it is reasonable to assume that cooperative effects involving many more residues would be necessary in the case of sodium pectate to lead to either multi-stranded or helix–helix interactions. Extended

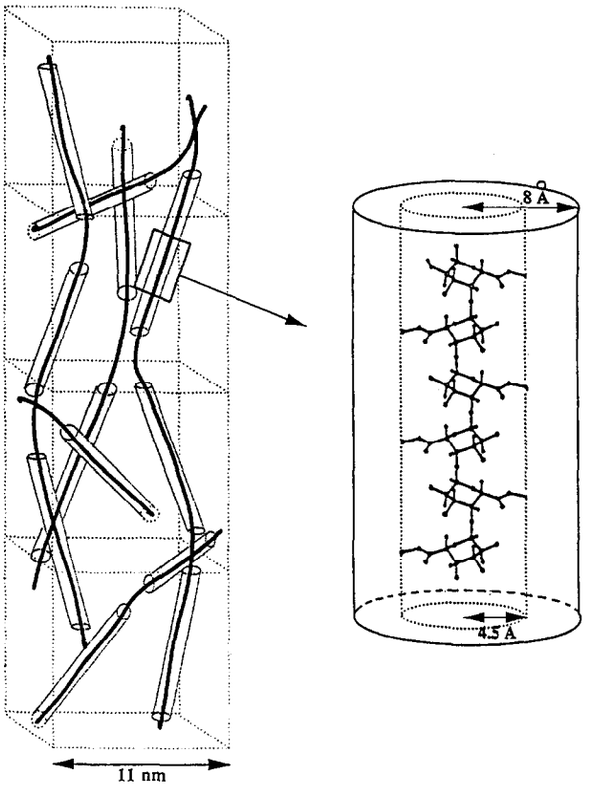

Fig. 5. Schematic representation of the secondary structure of a solution of sodium pectate at very low salt concentration. An expansion of the helical segment has been given on the right.

domains of junction zones are not compatible with the detection of more than 80% of the macromolecule by liquid-state NMR spectroscopy. Although it is not possible to deny the existence of some domains containing aggregated species, the vast majority of the macromolecule is constituted by the helical segments whose geometry and motional properties were determined from ^{13}C relaxation data. Therefore, the average axial length of the helical segments of 13 nm, which corresponds to about 29 out of the 100 residues per molecule, must be related to the natural curvature of the polysaccharide helix. A schematic representation of sodium pectate which illustrates the structural features established by fitting the relaxation data has been given in Fig. 5.

In summary, it has been possible to characterize the secondary structure of aqueous sodium pectate based on multi-field ^{13}C relaxation data. The optimum motional model corresponded to anisotropic reorientation of two-fold helical segments containing 29 residues with a transverse radius of 0.8 nm and an average axial length of 13 nm. The diffusion-in-a-cone spectral densities afforded both the best fit to experi-

mental data and the most precise motional model. Once detailed models for a broad range of pectins (i.e. with varying degrees of methylation and substitution) in the isolated state have been established, it should be much easier to discern the interactions responsible for the junction zones or entanglement networks that constitute the gel-state.

Acknowledgements

This work was supported by a fellowship for L.C. from the French Ministère de la Recherche et de l'Enseignement Supérieur. The authors would like to thank Dr. I. Braccini of the CERMAV in Grenoble for the cartesian coordinates of the various polygalacturonan helices and Dr. B. Coutin of the Laboratoire de Chimie Macromoléculaire (URA 24) at Paris VI University for his guidance with the viscosity measurements. Fruitful discussions with Dr. S. Pérez and Dr. M. Axelos are gratefully acknowledged.

References

[1] M. McNeil, A.G. Darvill, S.C. Fry, and P. Albersheim, *Ann. Rev. Biochem.*, 53 (1984) 625–663.
[2] M. Yalpani, *Polysaccharides, Syntheses, Modifications and Structure / Property Relations*, Elsevier Science, Amsterdam, 1988.
[3] S. Cros, C. Garnier, M.A.V. Axelos, A. Imberty, and S. Pérez, *Biopolymers*, 39 (1996) 339–352.
[4] M.L. Fishman, P. Cooke, A. Hotchkiss, and W. Damert, *Carbohydr. Res.*, 248 (1993) 303–316.
[5] M.D. Walkinshaw and S. Arnott, *J. Mol. Biol.*, 153 (1981) 1075–1085.
[6] A.R. Kirby, A.P. Gunning, and V.J. Morris, *Biopolymers*, 38 (1996) 355–366.
[7] I.G. Plashchina, M.G. Semenova, E.E. Braudo, and V.B. Tolstoguzov, *Carbohydr. Polym.*, 5 (1985) 159–179.
[8] A. Cesaro, A. Ciana, F. Delben, G. Manzini, and S. Paoletti, *Biopolymers*, 21 (1982) 431–449.
[9] H. Grasdalen and B.J. Kvam, *Macromolecules*, 19 (1986) 1913–1920.
[10] G. Ravanat and M. Rinaudo, *Biopolymers*, 19 (1980) 2209–2222.
[11] B.A. Burton and D.A. Brant, *Biopolymers*, 22 (1983) 1769–1792.
[12] S. Cros, C. Hervé du Penhoat, N. Bouchemal-Chibani, H. Ohassan, A. Imberty, and S. Pérez, *Int. J. Biol. Macromol.*, 14 (1992) 313–320.
[13] M.C. Jarvis, *Plant, Cell Environ.*, 7 (1984) 153–164.
[14] R. Lapasin and S. Pricl, *Rheology of Industrial Polysaccharides, Theory and Applications*, Chapman and Hall, London, 1995.
[15] B. Manunza, S. Deiana, M. Pintore, and C. Gessa, *2nd Electronic Glycoscience Conference*, September 1996.
[16] P. Dais and A. Spyros, *Progr. NMR Spectrosc.*, 27 (1995) 555–633.
[17] S. Aldington, G.J. McDougall, and S.C. Fry, *Plant, Cell Environ.*, 14 (1991) 625–636.
[18] P. Dais, *Adv. Carbohydr. Chem. Biochem.*, 51 (1995) 63–131.
[19] A. Poveda, M. Bernabé, J.A. Leal, and J. Barbero, *2nd Electronic Glycoscience Conference*, September 1996.
[20] Q. Xu and C.A. Bush, *Glycobiology*, in press.
[21] M. Hricovini, M. Guerrini, G. Torri, S. Piani, and F. Ungarelli, *Carbohydr. Res.*, 277 (1995) 11–23.
[22] R. Roy, F.D. Tropper, A.J. Williams, and J.-R. Brisson, *Can. J. Chem.*, 71 (1993) 1995–2006.
[23] P. Dais, *Carbohydr. Res.*, 160 (1987) 73–93.
[24] P. Dais and R.H. Marchessault, *Macromolecules*, 24 (1991) 4611–4614.
[25] E. Tylianakis, P. Dais, I. Andre, and F.R. Taravel, *Macromolecules*, 28 (1995) 7962–7966.
[26] G. Lipari and A. Szabo, *J. Chem. Phys.*, 69 (1978) 1722–1736.
[27] R.E. London and M.A. Phillipi, *J. Magn. Reson.*, 45 (1981) 476–489.
[28] R. Dejean de la Batie, F. Lauprêtre, and L. Monnerie, *Macromolecules*, 21 (1988) 2045–2052.
[29] O.W. Howarth, *J. Chem. Soc., Faraday Trans. 2*, 75 (1979) 863–873.
[30] C. K. Hall and E. Helfand, *J. Chem. Phys.*, 77 (1982) 3275–3282.
[31] R.J. Wittebort and A. Szabo, *J. Chem. Phys.*, 69 (1978) 1722–1736.
[32] W.H. Press, B.P. Flannery, S.A. Teukolsky, and W.T. Vetterling, *Numerical Recipes in Pascal*, Cambridge University Press, Cambridge, 1989.
[33] J.W. Cooper, *Introduction to Pascal for Scientists*, Wiley, New York, 1981.
[34] J.A. Nelder and R. Mead, *Comput. J.*, 7 (1965) 308.
[35] D.J. Craik, A. Kumar, and G.C. Levy, *J. Chem. Inf. Comput. Sci.*, 23 (1983) 30–38.
[36] S.B. Engelsen, S. Cros, W. Mackie, and S. Pérez, *Biopolymers*, 39 (1996) 417–433.
[37] H.S. Owens, H. Lotzkar, T.H. Schultz, and W.D. Maclay, *J. Am. Chem. Soc.*, 68 (1946) 1628–1632.
[38] A. Isihara, *Adv. Polym. Sci.*, 5 (1968) 531–567.
[39] R.P. Lubianez, A.A. Jones, and M. Bisceglia, *Macromolecules*, 12 (1979) 1141–1145.
[40] H. Lamb, in *Hydrodynamics*, Dover, New York, 1945.
[41] S. Broersma, *J. Chem. Phys.*, 32 (1960) 1626–1631.
[42] G.S. Manning, *Biopolymers*, 26 (1987) 1–3.
[43] Y. Marcus, *Chem. Rev.*, 88 (1988) 1475–1498.
[44] G.S. Manning, *Acc. Chem. Res.*, 12 (1979) 443–447.
[45] A. Malovikova, M. Milas, M. Rinaudo, and R. Borsali, *ACS Symposium Ser. 548*, 33 (1992) 315–321.
[46] A.N. Lane, *Progr. NMR Spectrosc.*, 25 (1993) 481–505.
[47] S.B. Engelsen, C. Hervé du Penhoat, and S. Pérez, *J. Phys. Chem.*, 99 (1995) 13334–13351.

[48] L.E. Kay, L.K. Nicholson, F. Delaglio, A. Bax, and D.A. Torchia, *J. Magn. Reson.*, 97 (1992) 359–375.
[49] A.G. Palmer III, N.J. Skelton, W.J. Chazin, P.E. Wright, and M. Rance, *Mol. Phys.*, 75 (1992) 699–711.
[50] M. Hricovini and G. Torri, *Carbohydr. Res.*, 268 (1995) 159–175.
[51] G. Lipari and A. Szabo, *J. Am. Chem. Soc.*, 104 (1982) 4546–4559.
[52] N. Bouchemal-Chibani, I. Braccini, C. Derouet, C. Hervé du Penhoat, and V. Michon, *Int. J. Biol. Macromol.*, 17 (1995) 177–182.
[53] A. Perico, *Acc. Chem. Res.*, 22 (1989) 336–342.
[54] M.J. Gidley, *Macromolecules*, 22 (1989) 351.
[55] E.R. Morris, D.A. Powell, M.J. Gidley, and D.A. Rees, *J. Mol. Biol.*, 155 (1982) 507–516.
[56] D.A. Powell, E.R. Morris, M.J. Gidley, and D.A. Rees, *J. Mol. Biol.*, 155 (1982) 517–531.